BIRKHÄUSER

Tsunami Science Four Years after the 2004 Indian Ocean Tsunami

Part II: Observation and Data Analysis

Edited by
Phil R. Cummins
Laura S. L. Kong
Kenji Satake

Birkhäuser
Basel · Boston · Berlin

Reprint from Pure and Applied Geophysics
(PAGEOPH), Volume 166 (2009) No. 1/2

Phil R. Cummins
Geoscience Australia
P.O. Box 378
Canberra, ACT 2601
Australia
Email: phil.cummins@ga.gov.au

Kenji Satake
Earthquake Research Institute
University of Tokyo
1-1-1 Yayoi
Bunkyo-ku
Tokyo 113-0032
Japan
Email: satake@eri.u-tokyo.ac.jp

Laura S. L. Kong
UNESCO Intergovernmental Oceanographic
Commission (IOC)
International Tsunami Information Centre
737 Bishop Street
Suite 2200
Honolulu, HI, 96813
USA
Email: l.kong@unesco.org

Library of Congress Control Number: 2009920437

Bibliographic information published by Die Deutsche Bibliothek:
Die Deutsche Bibliothek lists this publication in the Deutsche Nationalbibliografie; detailed bibliographic data is available in the Internet at <http://dnb.ddb.de>

ISBN 978-3-0346-0063-7 Birkhäuser Verlag AG, Basel · Boston · Berlin

ISBN 978-3-0346-0063-7 e-ISBN 978-3-0346-0064-4

9 8 7 6 5 4 3 2 1 www.birkhauser.ch

Contents

Pure appl. geophys. 166 (2009) 1–7
0033–4553/09/010001–7
DOI 10.1007/s00024-009-0442-0

Pure and Applied Geophysics

Introduction to ''Tsunami Science Four Years After the 2004 Indian Ocean Tsunami, Part II: Observation and Data Analysis''

PHIL R. CUMMINS,[1] LAURA S. L. KONG,[2] and KENJI SATAKE[3]

Abstract—In this introduction we briefly summarize the fourteen contributions to Part II of this special issue on *Tsunami Science Four Years After the 2004 Indian Ocean Tsunami*. These papers are representative of the new tsunami science being conducted since the occurrence of that tragic event. Most of these were presented at the session: Tsunami Generation and Hazard, of the International Union of Geodesy and Geophysics XXIV General Assembly held at Perugia, Italy, in July of 2007. That session included over one hundred presentations on a wide range of topics in tsunami research. The papers grouped into Part II, and introduced here, cover field observations of recent tsunami's, modern studies of historical events, coastal sea-level observations and case studies in tsunami data analysis.

Key words: Tsunami, tide gauge, sea level, waveform inversion, seiche, harbor resonance, numerical modeling, post-tsunami survey, tsunami warning system, runup.

1. Introduction

During the years following the 2004 Sumatra-Andaman Earthquake and subsequent Indian Ocean Tsunami (IOT), the world experienced a remarkable series of great earthquakes. The 2004 event marked the beginning of a series of earthquakes off Sumatra that included three of the ten largest earthquakes recorded since 1900 (http://earthquake.usgs.gov). During the period 2004–2007, nine earthquakes of magnitude 8 or greater occurred in the Indian and Pacific Oceans; all of which generated tsunami's, of which six were large enough to cause damage. These events coincided with a period of rapid growth in tsunami science spurred by the IOT disaster, including an expansion in earthquake and tsunami observation platforms, as well as dramatic improvements in technology and field techniques. Many observational studies of these and other events were presented in the session: Tsunami Generation and Hazard, at the International Union of Geodesy and Geophysics XXIV General Assembly in Perugia, Italy, held in July of 2007. Over

[1] Geoscience Australia, GPO Box 378, Canberra, ACT 2601, Australia. E-mail: Phil.Cummins@ga.gov.au
[2] UNESCO IOC International Tsunami Information Centre, 737 Bishop St., Ste. 2200, Honolulu, Hawaii 96813, U.S.A, E-mail: l.kong@unesco.org.
[3] Earthquake Research Institute, University of Tokyo, 1-1-1 Yayoi, Bunkyo-ku, Tokyo 113-0032, Japan E-mail: satake@eri.u-tokyo.ac.jp

one hundred presentations were made at this session, spanning topics ranging from paleo-tsunami research, to nonlinear shallow-water theory, to tsunami hazard and risk assessment. A selection of this work is published in detail in the 28 papers of the special issue of Pure and Applied Geophysics.

In this introductory paper, we briefly discuss the papers in this second part of *Tsunami Science Four Years after the 2004 Indian Ocean Tsunami*. In Section 2 we discuss field observations of recent tsunamis, while Section 3 describes some modern studies of historical events. Section 4 discusses tide gauge observations and Section 5 data analysis case studies.

2. Field Observations of Recent Tsunamis

Each damaging tsunami resulting from the series of great tsunamigenic earthquakes that occurred in 2004–2007 was followed by one or more post-tsunami surveys, and reports on three of these surveys appear in this volume. Careful observations of actual tsunami impacts, such as those presented in these reports, are invaluable for understanding tsunami runup and inundation, validating numerical tsunami models, and for interpreting geological signatures of paleo-tsunamis. The studies described below demonstrate how post-tsunami field observations can be used to infer detailed characteristics of the causative tsunami, to determine what factors influence inundation and runup, and to inform tsunami warning procedures.

LAVIGNE *et al*. (2009) provided a comprehensive summary of three months of tsunami field surveys from Banda Aceh and Lhok Nga, Indonesia in the aftermath of the 2004 Indian Ocean tsunami. Runup, wave heights, flow depths and directions, event chronologies and building damage patterns, inundation maps, high-resolution digital elevation models were collected and compiled. They reported that approximately 10 separate waves affected the region, and that the largest runups measured about 35 m with a maximum of 51 m; the highest value measured in human history from a seismically-generated tsunami. The open-source database is being made available to the community under the cooperative French-Indonesian TSUNARISQUE program to assist in better calibrating numerical models.

MACINNES *et al*. (2009) reported the results of their post-tsunami field survey of the M_w 8.3 Kuril Earthquake, which occurred on 15 November 2006, in the middle of Kuril Islands. Fortunately, they visited the islands for a paleo-tsunami survey in the summer of 2006, three months before the earthquake, hence they could compare visual observations, photographs and measurements of topographic profiles taken before and after the tsunami. While the November 2006 earthquake was followed by the January 2007 earthquake, the tsunami from the latter was smaller than that from the former, hence the authors attributed the geological traces of tsunamis to the 2006 earthquake. They found that the tsunami heights strongly depended on the local topography, and averaged about 10 m with a maximum of more than 20 m. Wherever sand was available, it was brought inland and deposited with landward thinning and fining features. Similar tsunami deposits from previous earthquakes were also found. They also described significant coastal

erosion features, such as scours, soil stripping, rock plucking or cliff retreat, at places where the runup heights were more than 10 m.

The effects of the 2006 Kuril Earthquake were also experienced in the far field. DENGLER *et al*. (2009) reported on the impact of this event in Crescent City, California, where later-arriving maximum waves and strong currents in excess of 10 knots over an 8-hour period caused an estimated US $9.2 million of damage to harbor docks despite its arrival at low tide. Crescent City is known to be historically vulnerable to tsunamis because of its coastal and undersea morphology. As a result of the 2006 tsunami, and to advise coastal officials that local conditions can cause wave amplification and strong currents, the West Coast/Alaska Tsunami Warning Center redefined its Advisory to caution that coastal threats may still persist even though significant widespread inundation was not expected for all regions. The authors also emphasized the important role of awareness as being a key for tsunami safety, especially when only modest tsunamis are expected.

3. Modern Studies of Historical Events

Several papers in this volume address the need to understand historical events in order to correctly infer what implications they may have for tsunami hazard. Historical events are most often studied by combining field observations of the type described above, with numerical or laboratory modeling, which can elucidate their source mechanisms. As demonstrated in the papers described below, an accurate understanding of the source mechanisms of historical tsunami events is important for assessing the potential for the occurrence of similar events.

SULEIMANI *et al*. (2009) used a viscous slide model coupled with shallow water equations to successfully model landslides and the ensuing local tsunami waves in Resurrection Bay, a glacial fjord in south-central Alaska, after the M_w 9.2 1964 Prince William Sound earthquake. The numerical results, in good agreement with eyewitness reports and other observational data, showed that three underwater slope failures were the major contributors to the tsunami that attacked Seward, Alaska less than five minutes after the earthquake. Their modelling approach was shown to be a useful tool for estimating landslide tsunami hazard, and their work demonstrated the need to consider these hazards in Alaska fjords where glacial sediments are accumulating at high rates on steep underwater slopes.

FRITZ *et al*. (2009) summarized two- and three-dimensional physical laboratory experiments that used a pneumatic landslide tsunami generator to model the 1958 Lituya Bay landslide tsunami, resulting in the highest wave runup (524 m) in recorded history. State-of-the-art measurement techniques were used to measure and photograph the landslide-water impact and wave generation. The two-dimensional velocity vector field showed the impact to be divided into two stages: (a) Impact and penetration with flow separation, cavity formation, and wave generation, and (b) air cavity collapse with landslide run-out and debris entrainment. The results were compared with other predictive relationships for amplitude and height since no actual tsunami heights are

available. Because this landslide-generated tsunami exhibited strong energy directivity, a three-dimensional physical model was constructed, and the surface velocities measured for future validation and benchmarking, using detailed bathymetry in a three-dimensional numerical simulation.

YELLES-CHAOUCHE *et al.* (2009) investigated the tsunamis generated from the 1856 Djidjelli earthquakes. Historical seismic intensity and tsunami wave information, combined with seismicity over the past 30 years and bathymetric and seismic reflection lines collected in 2005, were used to characterize the seismotectonics of the region and to infer the source rupture of the main earthquake and tsunami source. The numerical model results showed that much of the eastern Algerian coast and Balearic Islands were affected, with a maximum wave height of 1.5 m near the harbor of Djidjelli. This event, together with the 2003 Bourmerdes tsunami, demonstrate that the Algerian margin hosts several active tsunamigenic faults that could cause damage to the western Mediterranean and Algerian coasts.

HIRATA *et al.* (2009) reviewed multiple occurrences of tsunamigenic earthquakes along the southern Kuril subduction megathrust; one of the few areas in the world where one can test the contention that earthquake rupture occurs along characteristic segments. Tsunami data, both historic (tide gauge, field measurements, and eyewitness observations) and prehistoric (tsunami deposits), are used to provide information on rupture extent. The authors' interpretation of past studies indicates that there is substantial variability of rupture from event to event, suggesting that the idea that earthquakes repeatedly rupture characteristic segments is an oversimplification.

4. Coastal Sea-level Gauge Observations of Tsunamis

Sea-level records from coastal tide gauge stations provide some of the most detailed information available on tsunami source signatures and tsunami interaction with shallow bathymetry. They therefore have great potential to improve our understanding of potential coastal impacts of future tsunami's. They are also a critical source of information for tsunami warning systems to confirm generation of a tsunami (though data from DART (Deep-ocean Assessment and Reporting of Tsunamis) buoys are also being used for this purpose). For these reasons, understanding the quality of data from coastal tide gauges and what influences the signals recorded on them is of great importance in both progressing tsunami science and supporting tsunami mitigation. Four papers in this special issue dealt with sea-level data recorded by coastal gauges, STEPHENSON and RABINOVICH (2009), NAMEGAYA *et al.* (2009), PATTIARATCHI and WIJERATNE (2009), and ABE (2009).

STEPHENSON and RABINOVICH (2009) compiled tsunami instrumental data recorded on the Pacific Coast of Canada in 1994–2007. During these 15 years, 16 tsunamis were recorded. Eleven of these were from distant sources around the Pacific Ocean and the 2004 Indian Ocean tsunami. Three were from local earthquakes in Canada and a regional event in California, and two were of meteorological origin. Through their analysis, they

found that the background noise level was very high at Langara point, the northernmost station of British Columbia and hence an important location for a tsunami warning system. The station was therefore moved to a more protected location.

NAMEGAYA *et al*. (2009) presented results of analyses of tide gauge response characteristics and their influence on tsunami measurements. Following on from a study by SATAKE *et al*. (1988), in which tide gauge response characteristics were measured for tide gauge stations in northeast Japan, the authors made similar measurements for tide gauge stations located on the Japan Sea coast. The paper presented a thorough investigation of tide gauge response and corrections for these stations, showing that there was a wide variety of behavior between tide gauges. The results have the potential to facilitate analyses of tsunamis in the Sea of Japan, particularly the tsunami caused by the 2007 Niigataken Chuetsu-oki earthquake.

PATTIARATCHI and WIJERATNE (2009) presented summaries of sea-level records from three Sri Lanka and eleven Western Australia stations that recorded Indian Ocean tsunamis between 2004 and 2007. In comparing the station records, they showed that although the relative magnitude of the tsunami's varied due to the differences in the tsunami source, tsunami behavior at each station was similar and was affected by local and regional topography. Sea-level records from stations on the western side of Sri Lanka clearly showed reflections from the Maldives that arrived 2–3 hours after the first tsunami wave. Similarly, reflections from the Mascarene Ridge and/or Madagascar were observed about 15 hours after the first wave in records in western Australia. Tsunami waves also excited oscillations, or seiches, at a local resonance frequency that is related to the fundamental period of the offshore shelf.

ABE (2009) discussed the relation between resonant frequencies of Japanese ports and dominant periods of recent tsunamis (in 1983 and 1993) in the Japan Sea. The author measured sea level at 55 Japanese ports in comparatively calm conditions using a pressure gauge, and estimated the natural periods of harbor resonances (seiches) from the maximum spectral amplitudes. These were compared with similar analyses applied to coastal tide gauge recordings of the 1993 Hokkaido Nansei-oki and the 1983 Nihonkai Chubu-oki tsunamis. The author was able to conclude that natural oscillations were excited during the tsunamis. These new data on natural periods are an important contribution to the understanding of tsunami hazard in the bays along the Japan Sea coast.

5. Data Analysis Case Studies

The heightened tsunami activity during the period 2004–2007 contributed substantially to the pool of observational data on tsunami's, and this has spurred the development of new data analysis techniques, and increased the number of available case studies against which existing techniques could be benchmarked. The studies described below detail how this has led to improved understanding of the effects of source and bathymetry on tsunami waveforms and travel times.

BABA *et al.* (2009) investigated the degree to which finite fault inversions of seismic data for earthquake rupture patterns can be used to predict far-field tsunamis. They based their case study on the M_w 8.3 Kuril subduction zone earthquake of 15 November, 2006, which was the first teletsunami to be widely recorded by bottom pressure recorders deployed in the northern Pacific Ocean. Since these observations are not subject to the sensitivity to shallow bathymetry that introduces considerable uncertainty into coastal tide gauge measurements, any discrepancy between observed and predicted tsunami waveforms could be confidently ascribed to the source model. BABA *et al.* (2009) found that the source model obtained from seismic data, especially when seismic surface wave data are used, could be used to predict the tsunami waveforms with sufficiently high precision that they could be used in a joint inversion to better constrain earthquake source properties such as rupture velocity. The potential for use of such seismic models in a tsunami warning system to rapidly forecast teletsunami waveforms is discussed.

HÉBERT *et al.* (2009) compared several methods for characterizing the earthquake source of the M_w 8.0 2007 Peru earthquake, and then used them to model the tsunami in the far field in Nuku Hiva, Marquesas Islands, French Polynesia. A quick moment tensor inversion method (Preliminary Determination of Focal Mechanism, PDFM), available about 30 minutes after the earthquake, using seismic surface waves, gave a tsunami source that predicted far-field wave heights that were in good agreement over the first 90 minutes of tsunami wave arrivals. In contrast, the tsunami source from seismic body-wave inversion, while providing details on fault slip distribution and magnitude, produced far-field tsunami waves that were too small, thus confirming that tsunami waves are substantially more influenced by the earthquake's lower frequency components. The authors concluded that the PDFM method, complemented by inversions of the DART tsunami data, showed promise as an efficient, fast inversion method that can produce a realistic source permitting more accurate far-field wave forecasts to be calculated and used in tsunami warning applications.

WESSEL (2009) compared tsunami travel times reported in the literature with times predicted using the standard Huygens method. Over 1500 records from 127 earthquakes around the Pacific Ocean were compared. He first found large outliers in reported travel times; aside from obvious clerical errors, these outliers may be attributed to first arrivals that were missed because of their small amplitude, or to incomplete bathymetry data. Robust statistical analysis indicates that the median difference between data and predictions was less than 1 min, with an absolute deviation of 33 min. Fine bathymetry data with 2 min gridding yielded better results than a coarser 5 min grid.

Acknowledgments

Most of the papers included in this volume were presented in the tsunami session at the 2007 IUGG meeting held in Perugia, Italy. We thank all the participants who made that session such a success. We also thank the reviewers of each paper for their time and efforts, and Renata Dmowska and the editorial staff at Springer for their patience and support.

REFERENCES

ABE, K. (2009), *Excitation of resonant modes along the Japanese coast by the 1993 and 1983 tsunamis in the Japan Sea*, Pure Appl. Geophys. *166*(1–2), 117–130.

BABA, T., CUMMINS, P.R., THIO, H.K., and TSUSHIMA, H. (2009), *Validation and joint inversion of teleseismic waveforms for earthquake source models using deep ocean bottom pressure records: A case study of the 2006 Kuril megathrust earthquake*, Pure Appl. Geophys. *166*(1–2), 55–76.

DENGLER, L., USLU, B., BARBEROPOULOU, A., YIM, S.C., and KELLY, A. (2009), *The November 15, 2006 Kuril Islands-generated tsunami in Crescent City, California*, Pure Appl. Geophys. *166*(1–2), 37–53.

FRITZ, H.M., MOHAMMED, F., and YOO, J. (2009), *Lituya Bay landslide impact generated mega-tsunami: 50th anniversary*, Pure Appl. Geophys. *166*(1–2), 153–175.

HÉBERT, H., REYMOND, D., KRIEN, Y., VERGOZ, J., SCHINDELÉ, F., ROGER, J., LOEVENBRUCK, A. (2009), *The 15 August 2007 Peru earthquake and tsunami: Influence of the source characteristics on the tsunami heights*, Pure Appl. Geophys. *166*(1–2), 211–232.

HIRATA, K., SATAKE, K., TANIOKA, Y., and HASEGAWA, Y. (2009), *Variable tsunami sources and seismic gaps in the southernmost Kuril Trench: A review*, Pure Appl. Geophys. *166*(1–2), 77–96.

LAVIGNE, F., WASSMER, P., GOMEZ, C., BRUNSTEIN, D., GRANCHER, D., PARIS, R., VAUTIER, F., SETIAWAN, A., CAHYADI, R., GUNAWAN, T., FACHRIZAL, FLOHIC, F., and DE COSTER, B. (2009), *Reconstruction of tsunami inland Propagation on December 26, 2004 in Banda Aceh, Indonesia, through field investigations*, Pure Appl. Geophys. *166*(1–2), 259–281.

MACINNES, B.T., PINEGINA, T.K., BOURGEOIS, J., RAZHIGAEVA, N.G., KAISTRENKO, V.M., and KRAVCHUNOVSKAYA, E.M. (2009), *Field survey and geological effects of the 15 November 2006 Kuril tsunami in the middle Kuril Islands*, Pure Appl. Geophys. *166*(1–2), 9–36.

NAMEGAYA, Y., TANIOKA, Y., ABE, K., SATAKE, K., HIRATA, K., OKADA, M., and GUSMAN, A.R. (2009), *In situ measurements of tide gauge response and corrections of tsunami waveforms from the Niigataken Chuetsu-oki Earthquake in 2007*, Pure Appl. Geophys. *166*(1–2), 97–116.

PATTIARATCHI, C.B., and WIJERATNE, E.M.S. (2009), *Tide gauge observations of the 2004–2007 Indian Ocean tsunamis from Sri Lanka and western Australia*, Pure Appl. Geophys. *166*(1–2), 233–258.

SATAKE, K., OKADA, M., and Abe, K. (1988), *Tide gauge response to tsunamis: Measurements at 40 tide stations in Japan,* J. Marine Res. *46*, 557–571.

STEPHENSON, F. E. and RABINOVICH, A. B. (2009), *Tsunamis on the Pacific coast of Canada recorded in 1994–2007*, Pure Appl. Geophys. *166*(1–2), 177–210.

SULEIMANI, E., HANSEN, R., and HAEUSSLER, P. (2009), *Numerical study of tsunami generated by multiple submarine slope failures in Resurrection Bay, Alaska, during the Mw 9.2 1964 earthquake*, Pure Appl. Geophys. *166*(1–2), 131–152.

YELLES-CHAOUCHE, A.K., ROGER, J., DEVERCHERE, J., BRACENE, R., DOMZIG, A., HEBERT, H., and KHERROUBI, A. (2009), *The 1856 tsunami of Djidjelli (eastern Algeria): Seismotectonics, modelling and hazard implications for the Algerian coast*, Pure Appl. Geophys. *166*(1–2), 283–300.

WESSEL, P. (2009), *Analysis of observed and predicted tsunami travel times for the Pacific and Indian Oceans*, Pure Appl. Geophys. *166*(1–2), 301–324.

Pure appl. geophys. 166 (2009) 9–36
0033–4553/09/010009–28
DOI 10.1007/s00024-008-0428-3

Pure and Applied Geophysics

Field Survey and Geological Effects of the 15 November 2006 Kuril Tsunami in the Middle Kuril Islands

Breanyn T. MacInnes,[1] Tatiana K. Pinegina,[2] Joanne Bourgeois,[1]
Nadezhda G. Razhigaeva,[3] Victor M. Kaistrenko,[4] and
Ekaterina A. Kravchunovskaya[2]

Abstract—The near-field expression of the tsunami produced by the 15 November 2006 Kuril earthquake (M_w 8.1–8.4) in the middle Kuril Islands, Russia, including runup of up to 20 m, remained unknown until we conducted a post-tsunami survey in the summer of 2007. Because the earthquake occurred between summer field expeditions in 2006 and 2007, we have observations, topographic profiles, and photographs from three months before and nine months after the tsunami. We thoroughly surveyed portions of the islands of Simushir and Matua, and also did surveys on parts of Ketoi, Yankicha, Ryponkicha, and Rasshua. Tsunami runup in the near-field of the middle Kuril Islands, over a distance of about 200 km, averaged 10 m over 130 locations surveyed and was typically between 5 and 15 m. Local topography strongly affected inundation and somewhat affected runup. Higher runup generally occurred along steep, protruding headlands, whereas longer inundation distances occurred on lower, flatter coastal plains. Sediment transport was ubiquitous where sediment was available—deposit grain size was typically sand, but ranged from mud to large boulders. Wherever there were sandy beaches, a more or less continuous sand sheet was present on the coastal plain. Erosion was extensive, often more extensive than deposition in both space and volume, especially in areas with runup of more than 10 m. The tsunami eroded the beach landward, stripped vegetation, created scours and trim lines, cut through ridges, and plucked rocks out of the coastal plain.

Key words: Tsunami, Kuril Islands, coastal geomorphology, tsunami deposit, tsunami erosion.

1. Introduction

A pair of tsunamigenic great earthquakes occurred seaward of the middle Kuril Islands in November 2006 and January 2007—one of the largest earthquake doublets on record (Ammon *et al.*, 2008). The 2006 earthquake occurred along the plate boundary,

[1] Department of Earth and Space Sciences, University of Washington, Seattle, WA 98195, USA. E-mail: macinneb@u.washington.edu

[2] Institute of Volcanology and Seismology, Far Eastern Branch Russian Academy of Sciences, 683006 Petropavlovsk-Kamchatskiy, Russia.

[3] Pacific Institute of Geography, Far Eastern Branch Russian Academy of Sciences, 690041 Vladivostok, Russia.

[4] Institute of Marine Geology and Geophysics, Far Eastern Branch Russian Academy of Sciences, 693022 Yuzhno-Sakhalinsk, Russia.

whereas the 2007 earthquake was produced by normal faulting on the outer rise, similar to the interpreted source of the 1994 Shikotan earthquake (HARADA and ISHIBASHI, 2007, and earlier references).

Everywhere the 2006 and 2007 Kuril tsunamis were measured, the 2006 tsunami was larger (National Geophysical Data Center, NGDC database). Moreover, the 1994 Shikotan tsunami was an average of 1.5 times larger than the 2007 tsunami on trans-Pacific tide gages (NGDC database). The records in the database, as well as arguments we make herein, lead us to interpret our surveyed tsunami effects in the middle Kurils as the product of the 2006 tsunami.

The 15 November 2006 middle Kurils tsunami was widely reported in the media to be small, a report based principally on its early expression in northern Japan, where later tsunami waves had tide-gage water heights[1] reaching 0.6 m. Tide-gage heights in Hawaii ranged up to 0.76 m, and on the far side of the Pacific, in Crescent City, California, a 0.88-m-high wave (1.76 m peak to trough) generated $700,000-$1 million worth of damage (KELLY, 2006) in the harbor. Tide-gage records from the southern Kurils include maximum water heights of about 0.8 m (Sakhalin Tsunami Warning Center), however, there are no stations in the middle Kurils. Local runup for this tsunami remained unknown until our surveys in summer of 2007 (preliminary results reported in LEVIN *et al.,* 2008). No one lives in this remote area and logistics for visiting the islands are complex and expensive.

Two expeditions sponsored by the Institute of Marine Geology and Geophysics, Yuzhno-Sakhalinsk, Russia (IMGG) and the NSF-funded Kuril Biocomplexity Project (KBP) worked together in the middle Kurils in July and August 2007, to survey inundation, runup and geomorphic effects of the 2006 tsunami. Inundation and runup are standard descriptions of tsunami size and report the tsunami's maximum inland distance and the elevation of that position, respectively, for any given stretch of coastline (FARRERAS, 2000). Surveys of geomorphic impacts of tsunamis are less standardized and can include field descriptions or measurements of erosion, deposits, and other tsunami effects. In 2007, a total of four working groups documented tsunami effects at 130 locations in 11 bays, over a distance of about 200 km, along the rupture zone of the 15 November 2006 and 13 January 2007 earthquakes. Several members of the 2007 expeditions, including most of the authors, had surveyed parts of these islands in the summer of 2006, under the aegis of the KBP. Our prior surveying provided a remarkable opportunity to make direct measurements and comparisons, at the same time of year, of shorelines before and after the tsunamis.

2. 15 November 2006 and 13 January 2007 Earthquakes and Tsunamis

The two middle Kuril great earthquakes of 2006 and 2007 filled a seismic gap (Fig. 1). Previously, a large earthquake had not occurred in the middle Kurils Islands in at

[1] "Water height" is the term used in the NGDC catalogue for vertical deviation from zero, which is approximately equal to amplitude, which in turn is half the trough-to-peak wave height.

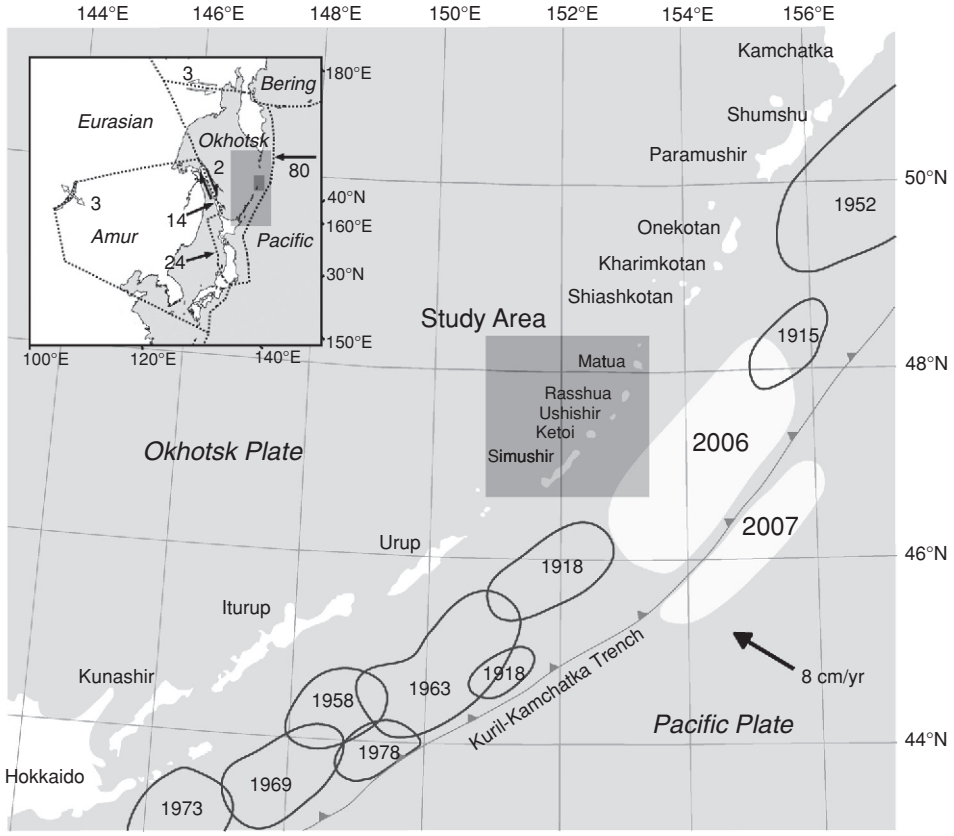

Figure 1
Tectonic setting of the Kuril Islands. Includes all historical tsunamigenic earthquakes with known source regions. Inset in the upper left: Plate tectonic map of the region including plate motions, after APEL *et al.* (2006). Measured plate motions are in mm/yr.

least 150 years—a previous event believed to have occurred along the middle Kurils (LAVEROV *et al.*, 2006), was an earthquake and tsunami experienced by Captain Snow off Simushir Island in 1780 (SNOW, 1910). The region had been interpreted as a seismic gap by Fedotov as early as 1965. However, there had been recent speculation as to whether this segment was slipping quietly (e.g., KUZIN *et al.*, 2001; SONG and SIMONS, 2003). Our paleotsunami field studies in the summers of 2006 and 2007 agree with the seismic-gap hypothesis (see below), as also confirmed by the recent earthquake doublet.

The 2006 earthquake released more total energy and lasted longer, whereas the 2007 earthquake had a higher peak energy release (AMMON *et al.*, 2008). The 15 November 2006 earthquake commenced at 11:14 UTC, according to the U.S. Geological Survey, at a depth of $\sim$30 km on the subduction zone. The epicenter for 2006 was off Simushir Island, and propagation proceeded northward (JI, 2006; VALLÉE, 2006; YAGI, 2006). The

13 January 2007 earthquake, which commenced at 04:23 UTC at a crustal depth of ~10 km, was a normal-faulting, outer-rise event on the Pacific Plate, directly east of the Kuril-Kamchatka trench (JI, 2007; VALLÉE, 2007; YAGI, 2007). According to the U.S. Geological Survey, the epicenter was approximately 100 km ESE of the 2006 event. Global CMT solutions record the 2006 event as a M_W 8.3 and the 2007 event as a M_W 8.1, although analysis of tsunami waveform inversions by FUJII and SATAKE (2008) suggest that M_W 8.1 and M_W 7.9 for 2006 and 2007, respectively, are more appropriate. AMMON *et al.* (2008) calculate M_W 8.4 for 2006 and M_W 8.1 for 2007 based on source radiation characteristics.

Both the 2006 and 2007 earthquakes produced measurable tsunamis around the Pacific Rim, although 2007 was smaller at every reported location. Observations from 113 locations for the 2006 event, and 35 locations for 2007, are archived in the National Geophysical Data Center (NGDC), Global Tsunami Database, and a few non-overlapping points in the Novosibirsk Tsunami Laboratory (NTL) Historical Tsunami Database.[2] Reported 2006 tide-gage water heights range from < 0.1 m at several locations to values of 0.4 to 0.9 m at some stations in the southern Kurils, Japan, New Zealand, Chile, the Marquesas, Hawaii, the West Coast of the U.S., and the Aleutians. Of the records of the 2007 tsunami, the maximum reported tide-gage water heights are about 0.4 m at Malokurilsk (RABINOVICH *et al.*, 2008) and Chichijima Island, ~0.3 m at Shemya in the Aleutians, and ~0.25 m at Port Orford and Crescent City, U.S.A. The closest measurements of the 2007 Kuril tsunami on a directed path of the earthquake, in Hawaii, are an average of 3.5 times less than those of the 2006 Kuril tsunami.

3. Neo-Tectonic and Geomorphic Setting

The Kuril Islands are a volcanic arc associated with subduction of the Pacific Plate under the Okhotsk Plate (Cook *et al.*, 1986) along the Kuril-Kamchatka trench. Subducting crust is ~100 million years old, and the convergence rate is 8 cm/yr (DEMETS *et al.*, 1990), excluding Okhotsk Plate motion (APEL *et al.*, 2006). The Kuril Island chain includes more than 25 islands with roundly 30 active volcanoes and many prominent volcanic edifices (GORSHKOV, 1970; MELEKESTSEV, 1980).

The islands surveyed in both 2006 and 2007, Simushir to Matua islands (Fig. 2), are morphologically different than islands to the north and south. The middle Kurils span a ~20° bend in the arc and are smaller and more widely spaced than the northern and southern islands. Primarily, the middle islands are single or multiple volcanic edifices, with the most common coastline being steep sea cliffs. Study sites fall into two broad geomorphologic categories—bouldery pocket beaches or broad embayments with gravelly to sandy shorelines (Figs. 2 and 3). The coastal plain in most field locations

[2] Note that the NGDC database reports water heights above zero, whereas the Novosibirsk database reports peak-to-trough wave heights. We are using only tide-gage records for this comparison.

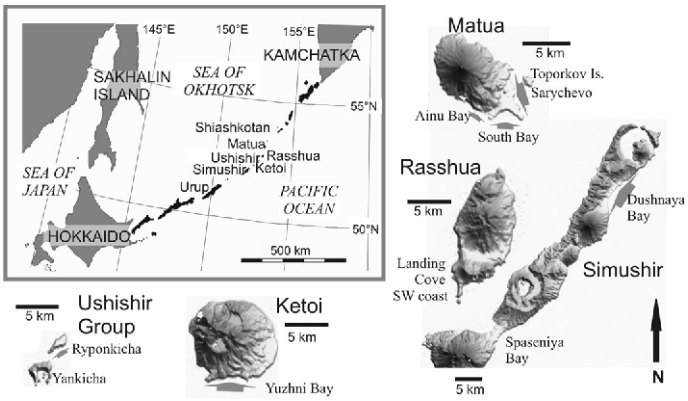

Figure 2
Overview of the basic morphology of the islands surveyed in 2007, including site names from Table 1. The scale bar for each island is 5 km.

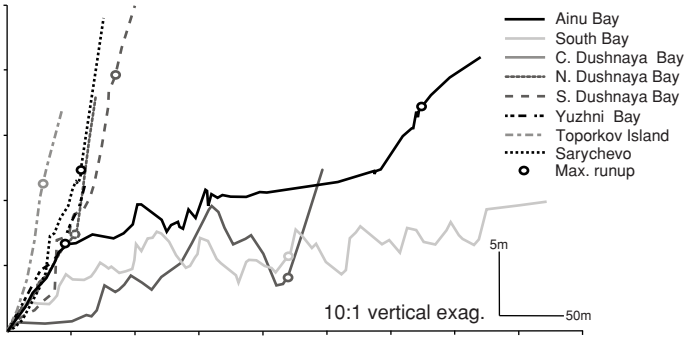

Figure 3
Example profiles that illustrate differences among short, steep coastlines (dashed lines) and broad coastal plains (solid lines). C (Central) Dushnaya Bay is an example of a profile in Table 1, where maximum runup elevation is less than the maximum elevation on the profile.

is backed by a cliff or steep slope. The largest embayments have up to 500 m of sandy coastal plain before this cliff, although more than half of the profiles measured were along rocky beaches with shoreline widths averaging around 50 m (Fig. 3).

4. Tsunami Survey Methods

Up to four teams operated simultaneously to measure topographic profiles, to record maximum runup and inundation, to collect tsunami-deposit samples and descriptions, and to make observations of erosion. Most sites visited in summer 2007 had been observed by team members previously, which helped us distinguish tsunami erosion and deposition

from other processes. Newly visited localities in 2007 include Spaseniya Bay on Simushir Island and Toporkov Island off Matua Island (Fig. 2).

Except where noted in Table 1, we made all measurements with a tripod, level and rod, with an individual measurement error of 0.3 cm vertically and 30 cm horizontally. This error does not accumulate in a given segment (until the level is moved), so that cumulative vertical error is less than 30 cm and horizontal error generally less than a few meters; each measurement was checked for error in the field. In a few cases, we used a hand level and tape, with error of 2 cm vertically per measurement and about 5% error horizontally, the latter due to irregularities on the ground. Also, where slopes were steep, we converted taped measurements trigonometrically from on-the-ground to horizontal. Whenever possible, we also checked horizontal measurements with distances calculated from GPS points (Table 1).

We measured profiles to or from local sea level and in most cases corrected for tide at the time of measurement from local tide tables. Measurements were not corrected for tide at the time of the earthquake, which began about mid-tide on the flood phase, in a low-amplitude tidal cycle (less than 0.5 m), based on tide tables and nearby tide gages; storm waves were active at the same time. Tidal range is typically 0.5–1.5 meters, thus even without corrections, error in the elevation of mean sea level is slight relative to runup.

At nearly every location surveyed, we could find evidence for an inland limit of tsunami penetration. Our primary criteria for defining runup were lines of floatable debris—typically driftwood, cut wood, plastic bottles and floats, glass floats, and styrofoam. In regions with short grasses and flowers, debris lines were obvious, and often one measurement accurately reflected runup. Where floated debris was obscured by this year's growing vegetation so that a debris line was not clear, we bushwacked, traced debris through the vegetation, and measured multiple points along 10–50 lateral meters. Both individual measurements and averages are reported in Table 1 and summarized in Table 2 and Figure 4. Single pieces of debris, such as one plastic bottle, were not considered adequate, as these bottles can blow in the wind. We observed some movement of debris material by animals, such as foxes, but it was rare. With the exception of southern Urup (briefly surveyed) and a small abandoned camp on Matua, we have no evidence that people had visited these islands since our visit in summer 2006. In a few cases, we measured heights of draped grass and seaweed on shrubs, but such flow-depth indicators were rare. Corroborative evidence of runup, not used independently, included the limit of consistently seaward-oriented stems of tall grasses and flowers, the limit of sand and gravel deposits on top of turf and dead vegetation, and the elevation of fresh erosion of turf.

5. 2006 or 2007?

We assumed our maximum runup and inundation limits were due to the 2006, not 2007, tsunami partly based on survey and catalogue data. First, the 2007 tsunami was measured to be smaller at *every* catalogued location around the Pacific. At the closest

Table 1

Table of runup and inundation of localities surveyed for the 2006 Kuril tsunami

Locality name	Latitude of profile at shore*	Longitude of profile at shore*	Runup (m)[&]	# of runup readings	Standard deviation	Max. elevation on profile seaward of inundation (m)	Inundation range[%]	Method[#]
Spaseniya Bay-36	46.84520	151.89542	**1.3**	1	-	3.9	**172**-212	HL
Spaseniya Bay-37	46.83173	151.87659	**3.9**	1	-	4.4	**141**–180	HL
Spaseniya Bay-39	46.83411	151.87962	**2.3**	1	-	3.9	**127**–146	HL
Spaseniya Bay-78	46.85281	151.90750	**4.4**	1	-	no	**115**–140	HL
Spaseniya Bay-79	46.85087	151.90409	**6.2**	1	-	no	**59**–80	HL
Spaseniya Bay-77b	46.84178	151.89000	5.7	1	-	no	**54**–109	HL
Spaseniya Bay-82	46.83668	151.88249	7.2	1	-	no	**51**–75	HL
Dushnaya Bay-24	*47.07085*	*152.18777*	8.7	1	-	no	77	HL
Dushnaya Bay-54	*47.04769*	*152.16070*	11.7	1	-	no	44	HL
Dushnaya Bay-57	*47.04684*	*152.15963*	9.3	1	-	no	115–136	HL
Dushnaya Bay-100	47.07971	152.21016	**13.3**	1	-	no	68	TL,HLT
Dushnaya Bay-101	47.07880	152.20884	***8.8***	5	0.14	no	**39**–44	TL
Dushnaya Bay-102	47.07835	152.20566	***7.7***	8	0.85	no	**50**–51	TL
Dushnaya Bay-103	47.07818	152.20214	***10.8***	10	0.48	no	**46**–49	TL
Dushnaya Bay-104	47.07809	152.19888	***13.0***	7	0.52	no	52–**52**	TL
Dushnaya Bay-105	47.07754	152.19528	***15.5***	10	0.39	no	93–**102**	TL
Dushnaya Bay-106	47.07537	152.19476	***13.0***	10	1.32	no	**66**–70	TL
Dushnaya Bay-107	47.07312	152.19315	***15.3***	12	1.90	no	**74**–85	TL
Dushnaya Bay-108	47.07124	152.19088	***11.9***	9	0.44	no	**57**–61	TL
Dushnaya Bay-109	47.07039	152.18792	***9.1***	10	0.58	no	**56**–59	TL
Dushnaya Bay-1–2006	47.06971	152.18614	***10.6***	8	0.70	no	100–**102**	TL
Dushnaya Bay-110	47.06960	152.18429	***8.8***	11	0.36	no	**107**–114	TL
Dushnaya Bay-11	47.06582	152.17981	**8.2**	1	-	8.4	**109**–115	TL
Dushnaya Bay-10	47.06772	152.18230	**9.9**	1	-	no	**121**–133	TL
Dushnaya Bay-12	47.06393	152.17726	**6.9**	1	-	no	**115**–120	TL

Table 1 Continued

Locality name	Latitude of profile at shore*	Longitude of profile at shore*	Runup (m)[&]	# of runup readings	Standard deviation	Max. elevation on profile seaward of inundation (m)	Inundation range[%]	Method[#]
Dushnaya Bay-2-2006	47.06201	152.17549	**6.7**	1	-	7.7	122–**125**	TL
Dushnaya Bay-9	47.06094	152.17313	**7.3**	1	-	12.0	151–**154**	TL
Dushnaya Bay-8	47.05979	152.17162	**8.6**	1	-	11.4	118–**120**	TL
Dushnaya Bay-7	47.05807	152.16878	**6.3**	1	-	7.1	139–**139**	TL
Dushnaya Bay-6	47.05628	152.16650	**4.4**	1	-	10.1	**98**–106	TL
Dushnaya Bay-5	47.05409	152.16471	**11.3**	1	-	no	**128**–132	TL
Dushnaya Bay-3	47.04942	152.16235	**7.9**	1	-	no	123–**135**	TL
Dushnaya Bay-2	47.04530	152.15915	**12.4**	1	-	12.7	75–**92**	TL
Dushnaya Bay-1	47.04313	152.15841	**20.0**	1	-	no	**79**–83	TL
Yuzhni Bay-1a	47.29924	152.48283	***6.5***	7	0.37	no	**39**–52	HLT
Yuzhni Bay-1b	47.29868	152.48257	***6.9***	9	0.69	no	**75**	HL
Yuzhni Bay-1c	47.29834	152.48416	***6.7***	16	0.60	no	**51**–55	HLT
Yuzhni Bay-2	47.29807	152.48616	***7.4***	9	0.24	no	**54**–58	HLT
Yuzhni Bay-3	47.29640	152.49141	***6.5***	9	0.29	no	**27**–44	HLT
Yuzhni Bay-3b	47.29979	152.48218	**10.6**	1	-	no	**47**–63	HL
Yuzhni Bay-10b	47.29966	152.47368	**6.2**	1	-	no	37	HL
Yuzhni Bay-13	*47.29774*	*152.48760*	**9.2**	1	-	no	**43**–67	HL
Yuzhni Bay-10c	47.29659	152.49009	**6.7**	1	-	no	**38**–79	HL
Yuzhni Bay-59	47.30047	152.48114	**6.8**	1	-	no	**37**–67	HL
Yuzhni Bay-61	*47.30043*	*152.48006*	**6.3**	1	-	no	52	HL
Yuzhni Bay-62	47.30022	152.47934	**6.0**	1	-	no	**18**–37	HL
Yuzhni Bay-64	47.30033	152.47762	**10.4**	1	-	no	**22**–42	HL
Yuzhni Bay-67	47.30025	152.47754	**9.7**	1	-	no	34	HL
Yuzhni Bay-69	47.29968	152.47460	**7.9**	1	-	no	**35**–54	HL
Yuzhni Bay-71	*47.29966*	*152.47368*	**6.2**	1	-	no	37	HL
Yuzhni Bay-73	47.29960	152.47238	**6.8**	1	-	no	**23**–37	HL

Table 1 Continued

Locality name	Latitude of profile at shore*	Longitude of profile at shore*	Runup (m)[&]	# of runup readings	Standard deviation	Max. elevation on profile seaward of inundation (m)	Inundation range[%]	Method[#]
Yankicha-257	47.52596	152.82620	***13.5***	2	0.21	no	57–**70**	TL
Ryponkicha-238	47.53181	152.82719	***11.7***	4	0.60	no	**50**–52	TL
Ryponkicha-245	47.53244	152.82906	***11.2***	5	0.74	no	**55**–56	TL
Ryponkicha-253	47.53632	152.83617	***11.0***	5	0.72	no	**47**–50	TL
Ryponkicha-255	47.53742	152.84057	***7.4***	3	0.59	no	25–**30**	TL
Ryponkicha-249	47.53324	152.83098	***11.2***	3	0.39	no	**42**–46	TL
Ryponkicha-251	47.53508	152.83231	**12.0**	1	-	no	45–**55**	TL
Ryponkicha-285	47.53287	152.82868	**10.1**	1	-	no	**48**–60	HL
Ryponkicha-180	47.54934	152.85081	**5.7**	1	-	no	**47**–54	HL
landing cove-507	47.70630	152.96405	**9.4**	1	-	no	**53**–56	HL
SW coast-196	47.69963	152.96543	**4.2**	1	-	no	64	HL
SW coast-198	47.69893	152.96575	**5.0**	1	-	no	66	HL
Sarychevo-120	48.08416	153.26740	***12.0***	6	0.69	no	**68**–70	TL
Sarychevo-125	48.08323	153.26612	***11.8***	4	0.04	no	**103**–118	TL
Sarychevo-129	48.08123	153.26444	***10.6***	3	0.19	no	**42**–54	TL
Sarychevo-133	48.07906	153.26357	**12.5**	1	-	no	38–**44**	TL
Sarychevo-136	48.07707	153.26329	***10.7***	4	0.08	no	**34**–36	TL
Sarychevo-69	48.07510	153.26518	**12.6**	1	-	no	59–**94**	TL
Sarychevo-73	48.07340	153.26681	**18.1**	1	-	no	93–**106**	TL
Sarychevo-79	48.07098	153.26668	***19.0***	4	0.56	no	**45**–50	TL
Sarychevo-83	48.06911	153.26872	***16.8***	4	0.57	no	**35**–38	TL
Sarychevo-86	48.06642	153.26921	***15.7***	3	0.55	no	**52**–56	TL,HLT
Sarychevo-142	48.05172	153.27181	***14.3***	3	0.22	no	51–**54**	TL
Sarychevo-145	48.05310	153.26861	***12.2***	3	0.45	no	**55**–62	TL

Table 1 Continued

Locality name	Latitude of profile at shore*	Longitude of profile at shore*	Runup (m)[&]	# of runup readings	Standard deviation	Max. elevation on profile seaward of inundation (m)	Inundation range[%]	Method[#]
Sarychevo-147	48.05498	153.26675	**17.0**	1	-	no	**48**–49	TL
Sarychevo-149	48.05728	153.26618	**15.3**	1	-	no	**56**–60	TL
Sarychevo-152	48.05941	153.26706	**21.9**	1	-	no	**41**–48	TL
Sarychevo-154	48.06177	153.26918	**16.7**	1	-	no	**26**–46	TL
Sarychevo-157	48.06401	153.26918	***12.1***	3	0.70	no	69–**79**	TL
Sarychevo-170	48.04985	153.27407	**9.9**	1	-	no	**48**–55	HL
Sarychevo-167	48.04854	153.27534	**10.4**	1	-	no	**67**–71	HL
Sarychevo-166	48.04751	153.27489	**9.6**	1	-	no	56–**56**	HL
Sarychevo-165	48.04660	153.27397	**8.6**	1	-	no	**101**–122	HL
Sarychevo-164	48.04504	153.27429	**8.6**	1	-	no	**110**–124	HL
Sarychevo-162	48.04349	153.27506	**8.1**	1	-	no	109–**116**	HL
Sarychevo-161	48.04193	153.27764	**6.1**	1	-	no	**92**–108	HL
Sarychevo-160	48.04124	153.27865	**7.3**	1	-	no	**55**–56	HL
South Bay-216	48.04199	153.24922	**5.7**	1	-	7.6	**221**–223	TL
South Bay-222	48.03976	153.23971	***7.3***	2	0.65	7.0	**170**–174	TL
South Bay-224	48.04023	153.24302	**5.7**	1	-	5.9	215–**219**	TL
South Bay-228	48.04127	153.24595	**7.1**	1	-	no	**205**–233	TL
South Bay-148	48.04234	153.25296	**4.9**	1	-	9.9	**139**–174	HL
South Bay-149	48.04244	153.25585	**6.4**	1	-	8.2	**101**–134	HL
South Bay-150	48.04267	153.25930	**5.7**	1	-	6.4	**146**–176	HL
South Bay-151	48.04202	153.26372	**7.9**	1	-	8.1	**60**–95	HL
South Bay-152	48.04034	153.26773	**7.8**	1	-	no	**126**–147	HL
South Bay-153	48.03749	153.27090	**7.8**	1	-	no	**129**–254	HL
Ainu Bay-1–2006	48.04412	153.22497	**17.1**	1	-	no	**313**–327	HLT,2006
Ainu Bay-2-2006	48.04269	153.22650	***18.1***	6	0.19	no	**411**–432	TL

Table 1 Continued

Locality name	Latitude of profile at shore*	Longitude of profile at shore*	Runup (m)[&]	# of runup readings	Standard deviation	Max. elevation on profile seaward of inundation (m)	Inundation range[%]	Method[#]
Ainu Bay-145	48.04786	153.21894	**13.6**	1	-	no	**68**–121	HL
Ainu Bay-144	48.04707	153.22058	**14.0**	1	-	no	**119**–120	HL
Ainu Bay-143	48.04599	153.22315	**17.1**	1	-	no	**200**–244	HL
Ainu Bay-139	48.04537	153.22430	**18.1**	1	-	no	**288**–315	HL
Ainu Bay-130	48.04444	153.22463	**17.1**	1	-	no	**315**–356	HL
Ainu Bay-132	48.04284	153.22588	**18.3**	1	-	no	**376**–398	HL
Ainu Bay-133	48.04266	153.22644	**20.2**	1	-	no	**417**–503	HL
Ainu Bay-126	48.04154	153.22731	**20.8**	1	-	no	**315**–436	HL
Ainu Bay-142	48.03980	153.22876	**12.9**	1	-	no	**128**–164	HL
Toporkov-237	48.07637	153.28168	***10.0***	4	0.38	no	41	HLT
Toporkov-235	48.07510	153.28164	**11.3**	1	-	no	**26**–28	HLT
Toporkov-230	48.07375	153.28205	***9.9***	2	0.31	no	**27**–42	HLT
Toporkov-231	48.07213	153.28239	***9.3***	2	1.01	no	40–**40**	HLT
Toporkov-234	48.07238	153.28224	**8.0**	1	-	no	37–**42**	HLT

* *italic*- lat/long on profile

[&] **bold**- with tide correction; *italic*- average of readings

[%] regular- field measurement; **bold**- GPS distance between shore and max runup

[#] Method- TL Transit level and rod; HLT Hand level, rod and tape; HL Hand level, rod for elevation and distance; 2006 Used profile from 2006

Table 2

Average runup and inundation for each bay surveyed, differentiated by coastal geomorphology

Island	Locality name	Coastline type	Average runup (m)	Average inundation (m)
Simushir	Spaseniya Bay	coastal plain	4.86	111
Simushir	Dushnaya Bay	coastal plain	8.08	121
Simushir	Dushnaya Bay	short, steep	12.56	65
Ketoi	Yuzhni Bay	short, steep	7.50	39
Ushishir	Yankicha, Ryponkicha	short, steep	10.43	49
Rasshua	SW coast	short, steep	6.21	61
Matua	Sarychevo	coastal plain	9.23	108
Matua	Sarychevo	short, steep	13.36	57
Matua	South Bay	coastal plain	6.64	152
Matua	Ainu Bay	coastal plain	17.02	268
Matua	Toporkov	short, steep	9.84	35

locations with records, the 2007 tsunami was five times smaller than 2006 at Yuzhno-Kurilsk ($\sim$550 km to the south of our field area), and less than half as high at Malokurilsk ($\sim$500 km to the south of our field area) (refer to RABINOVICH *et al.*, 2008 for tide gage records). Furthermore, the M_w 8.1–8.3 1994 Shikotan tsunami—comparable in earthquake mechanism to 2007 and with a larger tsunami at most trans-Pacific sites—typically produced 3–8 m (max 10 m) runup in the Habomai island group, east of Kunashir Island, close to the trench, and 1–4 m (max 6 m) in the southern Kurils themselves (YEH *et al.*, 1995; KAISTRENKO, 1997; NGDC database). Average runup at sites parallel to the 1994 source is less than 5 m, whereas the average runup we surveyed parallel to the 2006 and 2007 ruptures (see below) is about 10 m.

In addition to arguments based on measured tsunami height and runup, we argue that the effects we surveyed were primarily from 2006 because local conditions on the islands were different for the two tsunamis. A Landsat image of Dushnaya Bay from 22 November 2006 shows extensive regions without snow at lower elevations. However, weather records from December 2006 and early January 2007 in Severo-Kurilsk and Yuzhno-Kurilsk (to the north and south of the field area) indicate that there would have been snow accumulation on the islands before the 2007 tsunami. Thus a frozen, snow-covered coast in January would be less susceptible to erosion and subsequent deposition, including movement of the beach debris we used to indicate runup. Tsunamis do not necessarily erode snow (particularly if ice-covered snow) during inundation (MINOURA *et al.*, 1996).

In Dushnaya Bay on Simushir Island, there was evidence along many profiles for a smaller wave postdating the largest wave to come ashore—we cannot confidently attribute this evidence to a later wave of 2006 or to 2007. For example, we observed a thin wrack line from a smaller wave ($\sim$3–5 m elevation). Also, we observed complex tsunami deposits on several profiles, where a patchy sand deposit (average maximum elevation 5 m) lay above a layer of flattened vegetation, which, in turn, covered a

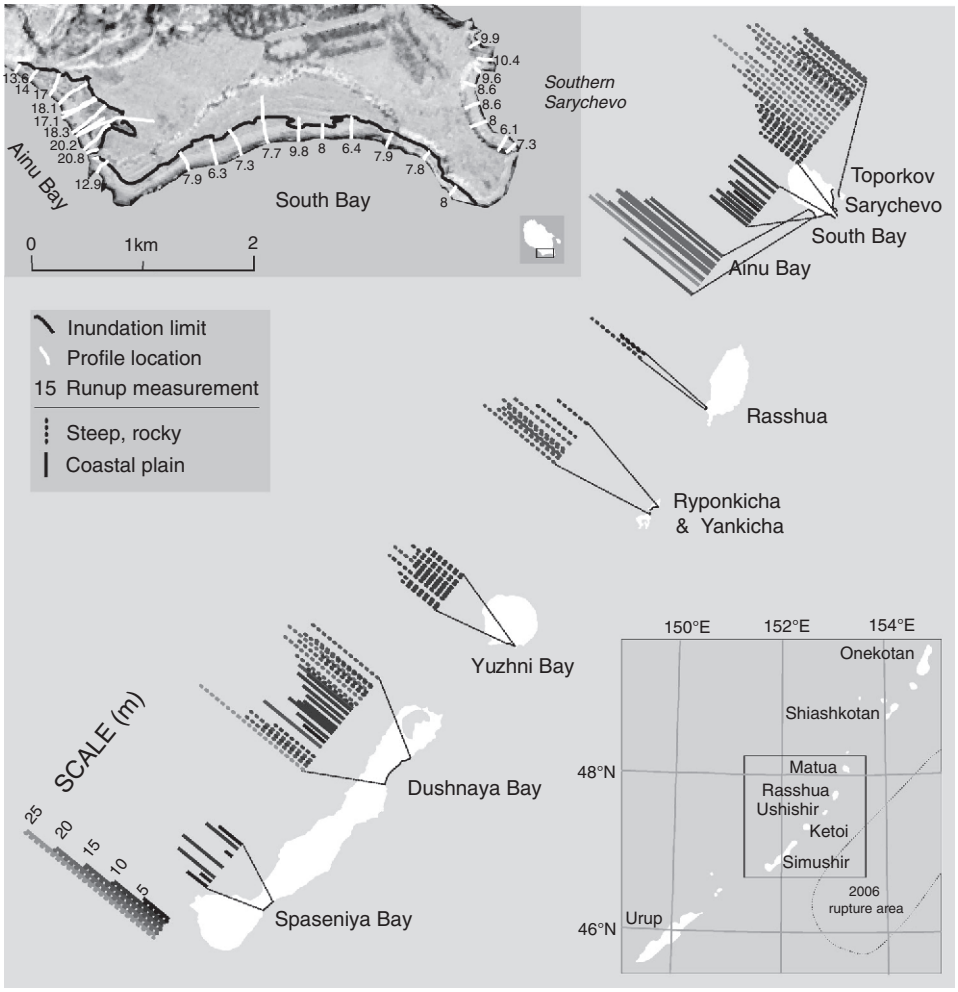

Figure 4
Summary of maximum runup of the 15 November 2006 tsunami, by location, for 130 field measurements. Values are categorized by the regional coastal geomorphology (refer to Fig. 3). Inset upper left: Detailed map of inundation and runup for southern Matua Island. Inset lower right: Location of the survey area.

continuous, coherent deposit. Such a depositional sandwich is what we expect from a second tsunami wave inundating over snow (Fig. 5), in which case these deposits would be from a smaller, 2007 tsunami.

6. Runup Observations and Inundation

Measured runup in the middle Kuril Islands (Simushir to Matua, about 200 km along strike) from the 2006 tsunami was typically 5–15 m, with a range of 2–22 m (Tables 1

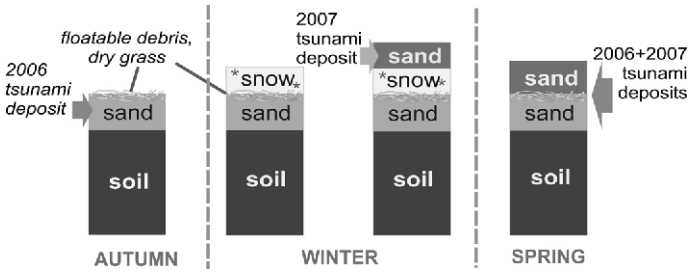

Figure 5
Schematic diagram of how the stratigraphic relationship of the 15 November 2006 and 13 January 2007 tsunami deposits appeared in the field. Snow that fell after the first tsunami would bury the 2006 deposit, floatable debris, and any vegetation still standing. The snow is not necessarily eroded in all locations by the second tsunami, and the resulting complex deposit has a thin layer of debris and vegetation in the middle.

and 2, Fig. 4), and a raw average of 10.2 m. Measured inundation varied from 20 to 500 m, with a raw average of 95 m. Average runup gives the tsunami a 3.85 on the S. Soloviev Tsunami Intensity scale (SOLOVIEV, 1972), the standard intensity scale used in the NGDC and NTL global tsunami databases:

$$I = {}^{1}/_{2} + \log_2 H_{av},$$

where H_{av} is the average height of the tsunami on the nearest coast. This scale does not take into account the distance along the shoreline of the surveyed region.

On some profiles (e.g., Central Dushnaya Bay profile in Fig. 3), seaward of maximum inundation, the tsunami over-topped beach ridges or sand dunes that were higher elevation than runup, which is by definition, elevation at maximum inundation. For these cases, Table 1 provides both runup and also maximum elevation along the profile, seaward of (maximum) inundation. Elevations along the profile do not take into account tsunami water depth, consequently the water height would have been even higher. We include the intra-profile data, in addition to runup and inundation, because they facilitate representation of the magnitude and behavior of the tsunami wave.

Variability in runup and inundation of the 2006 middle Kurils tsunami was in large part due to coastal geomorphology. Naturally, our longer inundation values are from lower, flatter coastal plains, and higher runup values generally from steep, protruding headlands (Table 2). In many of the cases we studied, the steep slope or cliff backing the coastal plain limited tsunami penetration. When a tsunami hits a reflector, such as a sea cliff, the energy not reflected back to the sea will be converted into vertical runup, increasing its height (BRIGGS *et al.*, 1996; PELINOVSKY *et al.*, 1999). Tsunami modeling will enable us to determine the degree to which coastal geomorphology, as well as bathymetry, affected tsunami runup; that work is in progress.

7. Tsunami Sediment Transport and Deposition

All affected shorelines showed evidence of erosion and deposition, and we made systematic measurements on many profiles (Table 3). Where loose sediment was available on the beach or in the nearshore, we observed deposits of sand, gravel, and cobbles on the coastal plain surface, burying turf and dead vegetation (Figs. 6B and D). Most deposits resemble sediment of the beach; more detailed analyses are forthcoming. In addition to beach sand and gravel, sediment also was derived from eroded scarps, from plucked turf and cobbles, and from artificial structures. Where the beach was composed of sediment larger than cobbles, no coherent, continuous deposit was present, although scattered boulders moved by the tsunami were common (see below). Where solid rock outcrop existed on the shore (observed on Ketoi and Matua), this rock was not noticeably affected by the tsunami.

We observed continuous tsunami sand sheets (e.g., Fig. 6D) in areas with sandy beaches, which also coincide with most low-relief profiles. As has been repeatedly seen elsewhere (c.f. SHI *et al.*, 1995; GELFENBAUM and JAFFE, 2003; BOURGEOIS, 2009), the 2006 Kurils tsunami deposits in these cases were typically thin (< 5 cm), thinning and fining landward. Over the 11 profiles where we made detailed observations, deposits were typically a few centimeters or less in thickness. Local variability in deposit thickness reflected previous topography; for example, a 0.5-cm-thick deposit locally thickened to 2–5 cm in a rodent burrow. In general, only close to the shore or in these locally low pockets did deposits exceed 5 cm in thickness.

Total volumes (average sediment thicknesses summed over distance) of sediment deposited ranged from 0.4 to 6.3 m^3/unit width (Table 3). The deposits used in these calculations were all on vegetated surfaces, with no evidence for subsequent erosion. Sediment volume is influenced by the amount of available sediment and by topographic variations controlling the velocity of the flow (GELFENBAUM and JAFFE, 2003). Profiles with less volume of sediment deposited had narrower and rockier beaches and lower runup. The largest volumes of sediment deposition came from profiles with severe beach erosion (see next section) and higher runup.

Sediment transport was not limited to sand- to cobble-sized material—across the middle Kurils, we found evidence of tsunami transport of boulders, ranging from 10's of cm to 3 m in diameter (Table 3). Moved boulders, known as *tsunami ishi* (KATO and KIMURA, 1983), were sourced from the nearshore, beach, coastal plain, and artificial structures (Fig. 6C). We easily identified tsunami *ishi* from the nearshore by recently deceased sea life on the boulders, such as attached seaweed, encrusted bryozoan communities, and kelp holdfasts. *Ishi* derived from artificial structures could generally be traced back to the dam or pier or other military structures from which they were derived. We commonly identified the source location of boulders from within the vegetated beach plain by the holes left behind (see the tsunami erosion section below for further discussion). Other than typically being clean and rounded, tsunami *ishi* that originated on the beach are associated with no identifiable characteristics so we only assume that if other

Table 3

Characteristics of onland effects of the 2006 Kuril tsunami for selected localities

Island	Locality name	Types of erosion*	Distance between erosion and max. inundation (m)	Sandy deposit noted?	Deposit volume (m^3/unit width)	Distance between deposition and max. inundation (m)	Tsunami *ishi*, minimum distance moved (m)	Evidence of smaller tsunami wave
Simushir	Dushnaya Bay-100	SB, SS	~0	yes	-	30	no	no
Simushir	Dushnaya Bay-101	SS, SC	10	yes	-	-	no	no
Simushir	Dushnaya Bay-102	SS, SC	13	yes	1.4	4	no	yes
Simushir	Dushnaya Bay-103	SS, SC	34	no	-	-	no	yes
Simushir	Dushnaya Bay-104	SB, SS, SC	10	yes	-	21	no	yes
Simushir	Dushnaya Bay-105	SB, SS, SC	14	yes	-	20	yes, 30	no
Simushir	Dushnaya Bay-106	SB, SS, SC, B	6.5	yes	-	-	yes	yes
Simushir	Dushnaya Bay-107	SB, SS, SC, P	13	no	-	-	yes	no
Simushir	Dushnaya Bay-108	SC, B, P	18	yes		10	yes	no
Simushir	Dushnaya Bay-109	SS, B, P	18	yes	0.4	13	yes, 10	no
Simushir	Dushnaya Bay-1-2006	SS, SC, B	1	yes	-	3	yes, 85	yes
Simushir	Dushnaya Bay-110	SS, SC, B	40	yes	-	-	no	yes
Simushir	Dushnaya Bay-12	SS, B	57	yes	0.9	3	no	yes
Simushir	Dushnaya Bay-2-2006	B	70	yes	1.2	2	no	yes
Simushir	Dushnaya Bay-9	SS, B	-	yes	3.0	0	no	no
Simushir	Dushnaya Bay-7	SS, B	-	yes	1.7	0	no	yes
Simushir	Dushnaya Bay-6	-	-	yes	1.2	0	no	yes
Simushir	Dushnaya Bay-2	SS, B	15	yes	0.9	3	no	no
Ketoi	Yuzhni Bay-1a	-	-	no	-	-	no	yes
Ketoi	Yuzhni Bay-1b	SB, SS	7.5	no	-	-	no	no
Ketoi	Yuzhni Bay-1c	SB, SS, SC	3.6	no	-	-	yes	no
Ketoi	Yuzhni Bay-2	SS	8	no	-	-	no	no
Ketoi	Yuzhni Bay-3	SC	0	no	-	-	no	no
Ushishir	Yankicha-257	SC	15	yes	-	9	no	no
Ushishir	Ryponkicha-238	SC, B	12	no	-	-	no	no
Ushishir	Ryponkicha-245	B	29	no	-	-	yes	no
Ushishir	Ryponkicha-253	SB	8	no	-	-	no	no
Ushishir	Ryponkicha-255	SS SC, SB	6	no	-	-	no	no
Ushishir	Ryponkicha-249	B	10	no	-	-	no	no

Table 3 Continued

Island	Locality name	Types of erosion*	Distance between erosion and max. inundation (m)	Sandy deposit noted?	Deposit volume (m^3/unit width)	Distance between deposition and max. inundation (m)	Tsunami *ishi*, minimum distance moved (m)	Evidence of smaller tsunami wave
Ushishir	Ryponkicha-251	SC	13	no	-	-	no	no
Rasshua	Landing Cove-507	SC	8	no	-	-	no	no
Matua	Sarychevo-120	SS, SC, B	11	yes	-	14	no	no
Matua	Sarychevo-125	SS, SC, B, P	9	yes	1.3	9	no	no
Matua	Sarychevo-129	T, SS, SC, B	2.5	no	-	-	yes	no
Matua	Sarychevo-133	T, SS, SC	3	yes	-	-	yes, 10	no
Matua	Sarychevo-136	T, SS	2	no	-	-	no	no
Matua	Sarychevo-69	T, SS, SC, B	5	yes	-	6	yes, 5	no
Matua	Sarychevo-73	T, SC, B	13	yes	-	34	yes, 40	no
Matua	Sarychevo-79	T, SC	5	no	-	-	yes, 20	no
Matua	Sarychevo-83	T, SS, SC	4	no	-	-	no	no
Matua	Sarychevo-86	SS, SC	4	yes	-	12	yes, 15	yes
Matua	South Bay-216	SS, B	60	yes	3.4	4	no	no
Matua	Ainu Bay-1-2006	SS, SC, B	10	yes	4.8	15	yes	yes
Matua	Ainu Bay-2-2006	SS, SC, B	6	yes	6.3	10	yes, 50	yes
Matua	Toporkov-237	T, SC	11	no	-	-	no	no
Matua	Toporkov-235	T, SC, B	2	no	-	-	no	no
Matua	Toporkov-230	T, SC	-	no	-	-	no	no
Matua	Toporkov-231	T, SC	3	no	-	-	no	no
Matua	Toporkov-234	T, SS, SC	1.5	no	-	-	no	no

*Types of erosion: T trim line; SB slope-base erosion; SS soil stripping; SC scours; B beach erosion; P rock plucking

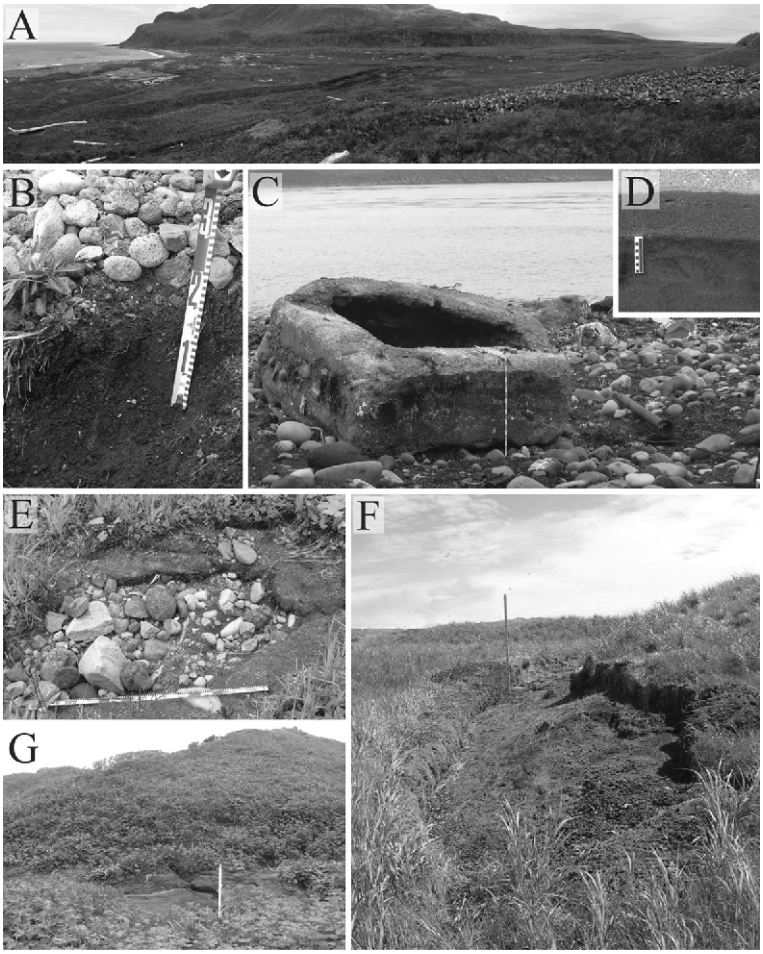

Figure 6

Deposition and erosion from the 15 November 2006 tsunami as observed in the middle Kurils. A: Ainu Bay, Matua, which experienced the maximum amount of inundation we observed (400–500 m). White flecks in the distance are large logs moved by the tsunami. B: A deposit of pebbles on top of soil and turf in Dushnaya Bay, Simushir (near profile 105). New vegetation is beginning to grow through. Measuring tape is 30 cm. C: A tsunami *ishi*, which was once an artificial structure offshore, with kelp holdfasts and bryozoan communities still attached. Measuring tape is 1 m. Sarychevo coast of Matua, profile 83. D: Continuous sand sheet from Ainu Bay, Matua, Profile 2. Here, the deposit is the thickest observed anywhere (at 20 cm thick) and is filling a drained lake bed. E: A scour pit in Dushnaya Bay, Simushir, Profile 106. Direction of flow was from right to left. Measuring tape is 1 m. F: Soil stripping in Ainu Bay, Matua, Profile 2. Turf and soil are still attached, but flipped over on the left (landward). The rod is 2 m high. G: Slope-base erosion in Dushnaya Bay, Simushir, Profile 107. The rod is 2 m high.

equivalent-sized boulders moved, the ones on the beach could have been moved. We recorded some tsunami *ishi* to have been transported at least > 85 m (Table 3), however we did not have time to conduct an exhaustive survey of all boulders transported.